

1-1-2002

## Resistivity Distribution in the Gediz Graben and its Implications for Crustal Structure

AYSAN GÜRER

ALAATTİN PİNÇE

ÖMER FEYZİ GÜRER

O. METİN İLKİŞİK

Follow this and additional works at: <https://journals.tubitak.gov.tr/earth>



Part of the [Earth Sciences Commons](#)

---

### Recommended Citation

GÜRER, AYSAN; PİNÇE, ALAATTİN; GÜRER, ÖMER FEYZİ; and İLKİŞİK, O. METİN (2002) "Resistivity Distribution in the Gediz Graben and its Implications for Crustal Structure," *Turkish Journal of Earth Sciences*: Vol. 11: No. 1, Article 2. Available at: <https://journals.tubitak.gov.tr/earth/vol11/iss1/2>

This Article is brought to you for free and open access by TÜBİTAK Academic Journals. It has been accepted for inclusion in Turkish Journal of Earth Sciences by an authorized editor of TÜBİTAK Academic Journals. For more information, please contact [academic.publications@tubitak.gov.tr](mailto:academic.publications@tubitak.gov.tr).

## Resistivity Distribution in the Gediz Graben and its Implications for Crustal Structure

AYSAN GÜRER<sup>1</sup>, ALAATTİN PİNÇE<sup>2</sup>, Ö. FEYZİ GÜRER<sup>3</sup> & O. METİN İLKIŞIK<sup>4</sup>

<sup>1</sup> Istanbul University, Engineering Faculty, Department of Geophysics, Avcılar, TR-34850  
İstanbul - TURKEY (E-mail: agurer@istanbul.edu.tr)

<sup>2</sup> Turkish Petroleum Corporation (TPAO), Mustafa Kemal Mahallesi, 2. Cadde, No. 86,  
TR-06520 Ankara - TURKEY

<sup>3</sup> University of Kocaeli, Engineering Faculty, Department of Geological Engineering, Vinsan,  
TR-41100 Kocaeli - TURKEY

<sup>4</sup> Anadolu Yerbilimleri, Perpa Ticaret Merkezi, A Blok, No. 157, Elektrokent, Şişli, İstanbul - TURKEY

**Abstract:** Preliminary results of resistivity distribution in the crust around the Gediz graben by the magnetotelluric (MT) measurements along two 73- and 16-km-long MT profiles (M1 and profile M2) are presented. Bostick depth transformation of the resistivity component of the MT data denoted a conductive zone at a depth of ~ 10 km. This zone may be related to crustal extension and high regional heat flow (50% higher than the world average). Preliminary interpretation based on one dimensional (1D) inversion result show that the thickness of sediments over the resistive basement changes from 950-3800 m along the profile M1. The relations between the trends of main structures in the region and abrupt lateral resistivity changes in the subsurface within the Gediz graben are discussed in the light of the residual apparent resistivity profiles.

**Key Words:** Gediz graben, magnetotelluric, resistivity, conductive lower crust

### Gediz Grabeninde Kabuk Yapısına İlişkin Özdirenç Dağılımı

**Özet:** Gediz grabeninde kabuk içinde özdirenç dağılımını gösteren ön sonuçlar sunulmaktadır. Özdirenç dağılımı, biri grabenin ana eksenine paralel, diğeri dik olan ve sırasıyla 73 km uzunluğundaki M1 ve 16 km uzunluğundaki M2 hatları boyunca alınan manyetotellurik (MT) verilerden elde edilmiştir. MT verilerin özdirenç bileşenine uygulanan Bostick derinlik dönüşümü, graben içinde 10 km derinlikte iletken bir kuşak göstermektedir. Bu kuşak, bölgedeki gerilmeli rejim ve yüksek bölgesel ısı akısı (dünya ortalamasından %50 daha yüksek) ile ilişkili olabilir. Bölgede jeolojik yapılar en az iki boyutlu olmasına karşın bir boyutlu ters çözümle bir ön değerlendirme dayanan yorumla bölgede çökel kalınlığının 950-3800 m olacak şekilde değişiklik gösterdiği söylenebilir. Gediz grabeni içinde yatay yöndeki ani özdirenç değişimleri Bostick dönüşüm kesitleri ve kalıntı özdirenç kesitleri kullanılarak izlenmiş ve bunların bölgedeki ana yapısal çizgisellikler ile ilişkili olabilecekleri düşünülmüştür.

**Anahtar Sözcükler:** Gediz grabeni, manyetotellurik, rezistivite, iletken alt kabuk

### Introduction

The geology of the western Anatolian grabens and the Gediz graben in particular have been studied in detail by several geologists during the last decade (Şengör 1987; Westaway 1994; Koçyiğit *et al.* 1999; Seyitoğlu & Scott 1992, 1994, 1996; Cohen *et al.* 1995; Yılmaz *et al.* 2000). According to these studies, extensional tectonic regimes have prevailed in western Anatolia and, as a result, the crust has thinned progressively in the region and eight major E-W- and twenty N-S- trending grabens have developed (Şengör 1987; Seyitoğlu 1997; Yılmaz *et*

*al.* 2000). However, there is no consensus on the timing of development or the relationships between the N-S and E-W graben groups in western Anatolia. Discussions have concentrated on the E-W-trending Gediz graben and the NE-SW-trending Gördes, Demirci and Selendi basins to the north of it. Seyitoğlu (1997), argued that the N-S and E-W grabens formed coevally as a result of ongoing NE-SW extension during the Early Miocene. However, Şengör (1987) suggested that N-S-trending basins contain older basin fill than the younger E-W-trending grabens. Koçyiğit *et al.* (1999) proposed an episodic, two-stage

graben model, with an intervening phase of short-term compression, for the evolution of the Gediz graben. A Miocene-Early Pliocene first stage occurred as a consequence of orogenic collapse, and a second phase of N-S extension originated from westward escape of the Anatolian block. Yılmaz *et al.* (2000) also suggested that the N-S-trending graben basins are older than the E-W-trending grabens, and also different times of development for these two systems; the N-S basins formed under an E-W extensional regime during the Early Miocene, whereas the present-day E-W-trending grabens developed in a NNE-SSW extensional regime that began during Late Miocene. These E-W grabens cut and displaced the N-S ones. According to this idea, the N-S grabens were continuous across the E-W graben areas before the development of the latter. If this hypothesis is valid, the remnants of N-S grabens and horsts should be trapped within the E-W graben basins.

In the centre of western Anatolia, the E-W-trending Gediz graben is, without question, one of the outstanding structures of this system with the ancient NE-SW-trending basins in the north (such as the Gördes, Demirci and Selendi basins). The Bozdağ horst and E-W-trending Büyük Menderes graben are located to the south of the 140-km-long Gediz graben. The high-grade metamorphic rocks of Menderes massif form the basement of the Gediz and neighbouring grabens and the intervening horsts separating the grabens.

Some regional-scale geophysical studies and several geothermal exploration programs have been carried out in the western Anatolian grabens during the last few decades (Başokur *et al.* 1996; Bayrak *et al.* 2001; MTA-General Directorate of Mineral Research and Exploration of Turkey; TPAO-Turkish Petroleum Corporation). One of these studies conducted by Geosystem, consisted of an MT survey in the Gediz graben as a part of the exploration program of TPAO (Turkish Petroleum Corporation MT measurements from 15 of the sites along 73 km of the major axis of the Gediz graben were made available to us). The MT site locations on profile M1 are shown on the 1:500,000 scale geological map of the Gediz graben and vicinity (Figure 1). These were used to map lateral variations in resistivity. The abrupt change in resistivity is mostly related to a similar change in lithology (fault or dike-like structures). So lateral resistivity changes along our E-W magnetotelluric profile may indicate possible hidden faults perpendicular (N-S) to

profile M1. The second MT line (profile M2) is a 16-km-long profile with six measurement sites, and crosses the Gediz graben around Salihli (Figure 1). The data from profile M2 reflects the conductivity distribution across the Gediz graben and the southern Bozdağ horst. MT data can also provide evidence for deeper crustal structures that may be relevant the high heat flow of the region.

Other geoelectric and geoelectromagnetic investigations have been carried out in the Gediz graben for geothermal prospecting by several companies (e.g., MTA and TPAO). Some of these measurements were from locations close to our MT profile M1 (Figure 1). We compared the 1D models obtained from these DC (Direct current) Schlumberger, CSAMT (Controlled Sourced Audiofrequency Magnetotelluric Method) and MT.

### Magnetotelluric Method

In the magnetotelluric (MT) method, the orthogonal components of the horizontal electric and magnetic fields induced by natural primary sources are measured simultaneously as a function of frequency. The source of energy for the magnetotelluric method is micropulsations having frequencies of less than 1 Hz. The predominant origin of the micropulsations is interaction of Earth's magnetopause with charged particles ejected from the sun. Electric- and magnetic-field components of these electromagnetic waves are measured with the horizontal pairs of orthogonal electric dipoles and magnetic sensors.

The orthogonal magnetic (H) and electric components (E) of natural fields can be related at each frequency by a tensor impedance (Z). The impedance tensor and impedance are given in equations (1) and (2), respectively.

$$\begin{aligned} E_x &= Z_{xx}H_x + Z_{xy}H_y \\ E_y &= Z_{yx}H_x + Z_{yy}H_y \end{aligned} \quad (1)$$

The notation  $Z_{ij}$  in equation (1) are the transfer functions called impedances. They are a measure of Earth's response to the magnetic fields in x and y directions. If the subsurface is homogeneous or horizontally stratified (one dimensional), the impedances  $Z_{xx}$  and  $Z_{yy}$  are equal to zero, and  $Z_{xy}$  and  $Z_{yx}$  impedances will be equal as below.

$$Z = \frac{\omega \mu_0}{k} = \frac{E_x}{H_y} = \frac{E_y}{H_x} \quad (2)$$

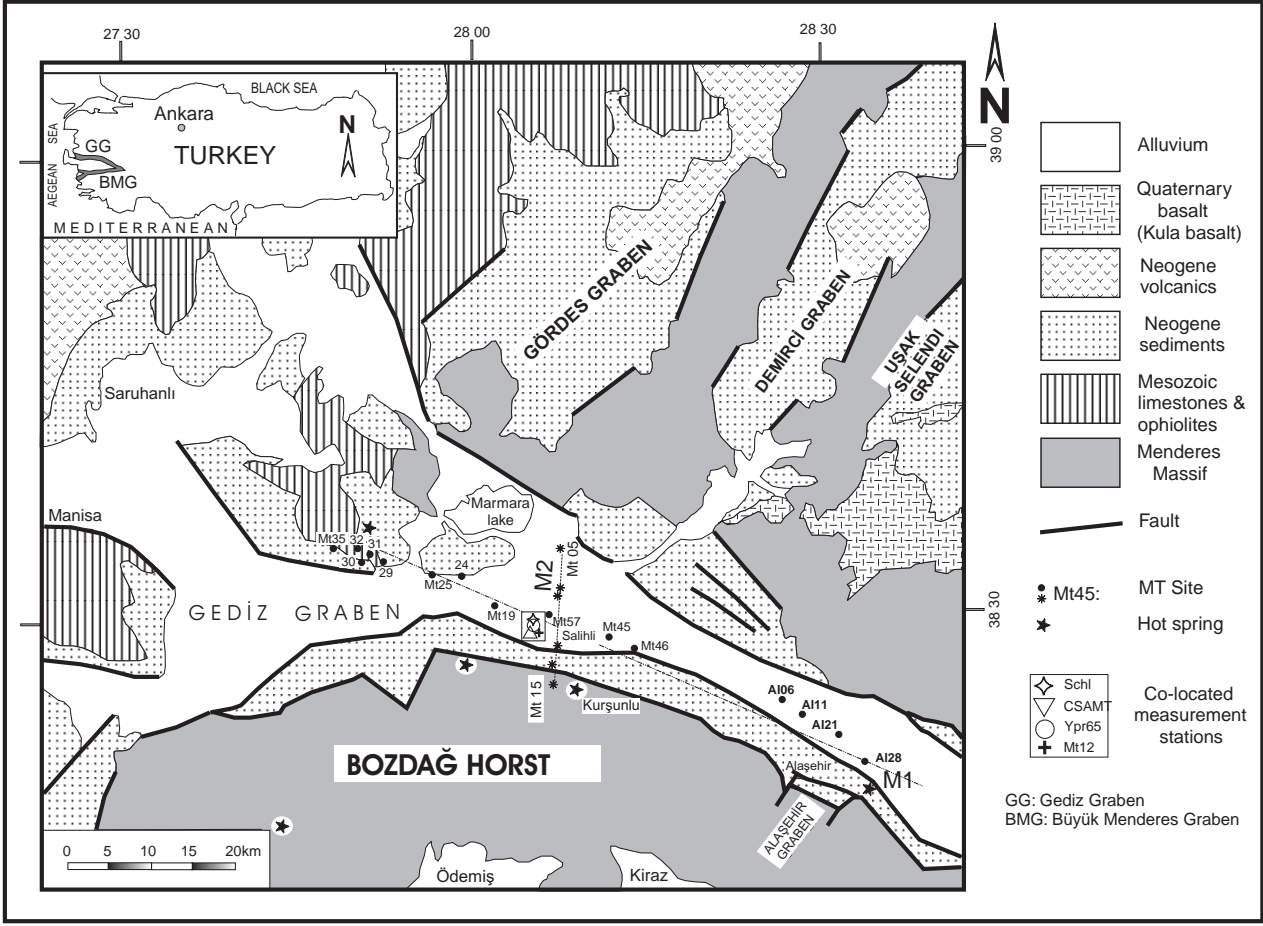


Figure 1. Geological map of the region (revised from MTA map 1964). Circles denote MT site locations.

Here,  $E$  and  $H$  are in  $mV/km$ , and  $nT$ , respectively,  $T$  is period in seconds,  $\omega = 2\pi f$  is angular frequency, and  $\mu_0$  is the magnetic permeability of the free space ( $4\pi \cdot 10^{-7}$  H/m).  $k$  is the propagation parameter and

$$k = (\omega\mu_0/2\rho)^{1/2}$$

The impedances are related to a complex measure of the Earth's resistivity. Apparent resistivity and impedance phase (as a function of frequency) are calculated in two orthogonal directions related to the two orthogonal measurement directions for any site (Cagniard 1953).

$$\begin{aligned} \rho_{XY} &= \left(\frac{1}{\omega\mu_0}\right) |Z_{XY}|^2 \\ \rho_{YX} &= \left(\frac{1}{\omega\mu_0}\right) |Z_{YX}|^2, \text{ ohm m} \end{aligned} \quad (3)$$

the phases of the impedance tensor are

$$\begin{aligned} \phi_{XY} &= \tan^{-1}\left(\frac{\text{im}Z_{XY}}{\text{re}Z_{XY}}\right) \\ \phi_{YX} &= \tan^{-1}\left(\frac{\text{im}Z_{YX}}{\text{re}Z_{YX}}\right), \text{ radian} \end{aligned} \quad (4)$$

If the Earth is homogeneous or horizontally layered (1D) the impedances, phases ( $\phi$ ) and resistivities in  $xy$  and  $yx$  directions will be equal (i.e., resistivity changes multidimensionally, 2D and 3D) otherwise they will have different values for the same site for the same measurement. One of the ways of understanding subsurface dimensionality is to calculate two parameters named tipper and skew. The magnetic components of MT fields are strongly affected by vertical contacts in subsurface. The horizontal magnetic components  $H_x$  and  $H_y$  can be related to the vertical magnetic component  $H_z$  as below:

$$H_z = AH_x + BH_y$$

A and B are complex transfer functions: The tipper is

$$T = (A^2 + B^2)^{1/2} \quad (5)$$

Tipper can be considered as the ratio of the induced vertical component to the total incident electromagnetic field. Any abrupt change in resistivity increases the vertical magnetic component, ( $H_z$ ) and the tipper(T). The tipper has a maximum value near a vertical contact and  $T=0$  for 1D earth. As a result, tipper can be considered a measure of two dimensionality. The second parameter, skew, is an indicator of three dimensionality and is calculated from the elements of impedance tensor as below.

$$S = (Z_{xx} + Z_{yy}) / (Z_{xy} - Z_{yx}) \quad (6)$$

Skew  $S=0$  for the one and two dimensional Earth and maximum for 3D Earth.

After calculating apparent resistivity and phases, the magnetotelluric data is presented as apparent resistivity and phase curves versus frequency for each site. Resistivity distribution as a function of depth can be calculated using Bostick transformation. This simple operator converts the frequency axis to the depth and apparent resistivities to the Bostick resistivities that are more closer to the real resistivities of the each layer. This transformation supplies a reasonable initial model for the inversion and an opportunity looking at the resistivity variation versus depth by a simple analysis before inverting the data. The Bostick resistivity ( $\rho_B$ ) and depth ( $d_B$ ) values are calculated using apparent resistivity and frequencies as below

$$\rho_B = \rho_a(f) \frac{(1-m)}{(1+m)} \quad (7)$$

where  $m$  is the trend of apparent resistivity and frequency curve

$$m = \frac{d(\log \rho_a)}{d(\log f)}$$

$$d_B = \left( \frac{\rho_a}{2\pi\mu_0 f} \right)^{1/2} = 356 \left( \frac{\rho_a}{f} \right)^{1/2} \text{ meter} \quad (8)$$

## Data Acquisition and Process

Data acquisition was carried out in 1989 by Geosystem and the Turkish Petroleum Corporation (TPAO). MT soundings were made using a Phoenix V5 digital system with 12-20 hour recording duration. The incoming data stream from the three magnetic and two electric field sensors was digitised and processed in real time; display of the output parameters allowed the operator to optimise lay-out and recording parameters. This resulted in good quality data especially in the frequency range 100 to 0.002 Hz of the overall frequency band extending between 320-0.00055 Hz.

The MT data is presented as apparent resistivity and phase pseudosections. Before presentation, the data is rotated to obtain  $0^\circ$  between the measurement axis and the strike direction (by Geosystem).

Small-scaled, local subsurface inhomogeneities or discontinuities in surface topography cause a shift in MT apparent resistivity values by the same multiplicative factor at all frequencies. So the apparent resistivity curves are moved uniformly up or down. The resulting interpretation of resistivity responses will have the correct structural shape, but the depths and resistivities of the layers will be in error. One method for measuring static shift is a controlled-sourced measurement of magnetic field by the Time Domain Electromagnetic Method (TDEM). Unlike the electric field, the magnetic field is unaffected by surface inhomogeneities. To obtain a complete undistorted model of the Earth deep MT soundings are shifted to combine shallow TDEM soundings (Sternberg *et al.* 1988). There is no significant topographic discontinuity at the surface along the main axis of the Gediz graben basin (M1 line direction), whilst the elevation differences in orthogonal directions are invariant along the main axis of the basin. Thus, no significant terrain distortion is expected in the MT data from the region. However, near-surface inhomogeneities caused some distortion of our data. We removed these static-shift effects by the technique mentioned above using the TDEM co-located measurements with our MT sites.

## Interpretation of Magnetotelluric Data

In this study, the MT data along the profile M1 in two orthogonal directions (N-S, xy; E-W, yx) is presented as

apparent resistivity and phase pseudo-sections in N-S ( $E_{\perp}$ ) and E-W ( $E_{\parallel}$ ) modes as a function of frequency in Figures 2a and 2b, respectively. The sedimentary units in the graben are characterised by low apparent resistivity values whereas the metamorphic basement of the graben reveals higher resistivities in both directions.

Bostick transformation was applied to the apparent resistivity data in both modes (i.e.  $E_{\perp}$  and  $E_{\parallel}$  modes) in order to obtain the approximate subsurface resistivity distribution as a function of depth. The Bostick pseudo-section is shown in Figure 2c. Bostick resistivity distribution shows that the undulating resistive basement is located at the different depths along the graben. In other words, basement topography is undulating. The lateral resistivity discontinuities in the Bostick pseudo-section along profile M1 indicates that at least a 2D character of geological structure is dominant in the region.

We also present the MT data as residual apparent resistivity profiles to clarify possible lateral resistivity boundaries. In this method, resistivity profiles are drawn for each frequency and the values of apparent resistivities at each station are normalised by dividing each of the  $\rho_a$  values by the  $\rho_{av}$  average for that profile. Residual resistivity gives deviation from the average regional resistivity for a certain site and the high or low values of it mostly indicates any lateral discontinuity in structure at this site. We have plotted the logarithmic values of  $\rho_a/\rho_{av}$  for each station along the profile. With this arrangement, conductive regions are indicated by negative values while resistive regions are indicated by positive values. This scheme facilitates the visualisation of the location of lateral geologic variations beneath the surface of profile M1. Residual apparent resistivity profiles are plotted in Figures 3 and 4 for N-S and E-W directions, respectively. The residual E-W polarization data show the considerable negative anomalies beneath the sites MT-30 and Al-06 at frequencies less than 0.28 Hz. Smaller positive anomalies are observed beneath MT-57 and MT-46. The profiles in the N-S direction show positive and negative anomalies at MT-31 and MT-30, respectively, and two clear positive and negative anomalies occur at the MT-46 and Al-06. The disturbances on residual apparent resistivity profiles cannot be associated with terrain or near-surface effects because they were corrected previously. These anomalies possibly indicate the presence of lateral discontinuities along the main axis of the graben.

Other geoelectrical and geoelectromagnetic measurements are available in the region around the Kurşunlu geothermal field (Figure 1). The skew and tipper analysis along the profile M1 indicated that there are no 2-3 dimensionality effects in this location (between the sites MT19 and MT57). Thus, 1D modelling at this site may be applicable. The 1D inversion results from these co-located MT soundings (at the sites MT-12, ypr-065) and CASMT and DC resistivity soundings are compared in Figure 5. Application of all of these methods revealed a conductive layer at depths of a few hundred meters that may be related to hydrothermal alteration zones of the Kurşunlu geothermal reservoir. The 1D inversion of the MT soundings (in  $E_{\parallel}$  mode, in EW) also revealed a low resistivity (10-20 ohm.m) zone at depth of 10 km in the crust. Our parameter analysis from 1D inversion of the MT responses from some sites (MT-29, 30, 24, 25) also revealed that the depth to this conductive layer is one of the well-resolved model parameters. The low resistivity at 10 km depth in the crust may be related to the high regional heat flow (İlkışık 1995; İlkışık *et al.* 1997).

Another 16-km-long MT line (M2) with six sites was conducted across the Gediz graben near Saliqli (Figure 1). Profile M2 crosses the Gediz graben and Bozdağ horst to the south. The resistivity data versus frequency in N-S and E-W directions and their Bostick resistivity-depth transformation pseudo-sections are shown in Figure 6. The low-resistivity sedimentary fill of the Gediz graben can be distinguished on the northern end of the section in Figure 6. The resistive massif rocks of the Bozdağ horst appeared at higher frequencies (or at the shallower depths) on the southern end of the sections.

The most striking feature along the M2 line is south of the Gediz graben. According to the Bostick depth transformation, there is a conductive zone at around the depth of ~10 km under the Bozdağ horst (Figure 6d). This depth value is very consistent with the depth to the conductive third layer in the 1D model results for the sites around Saliqli. This indicates the conductive lower crustal layer in the Gediz graben continues beneath the Bozdağ horst to the south. Unpublished MT data (MTA) along a line crossing the Bozdağ horst and northern NE-SW-trending horst-graben systems in the region also shows this conductive zone is present across the Bozdağ horst and absent to the north of the Gediz graben around the NE-SW Demircidağ horst and the Gördes graben.

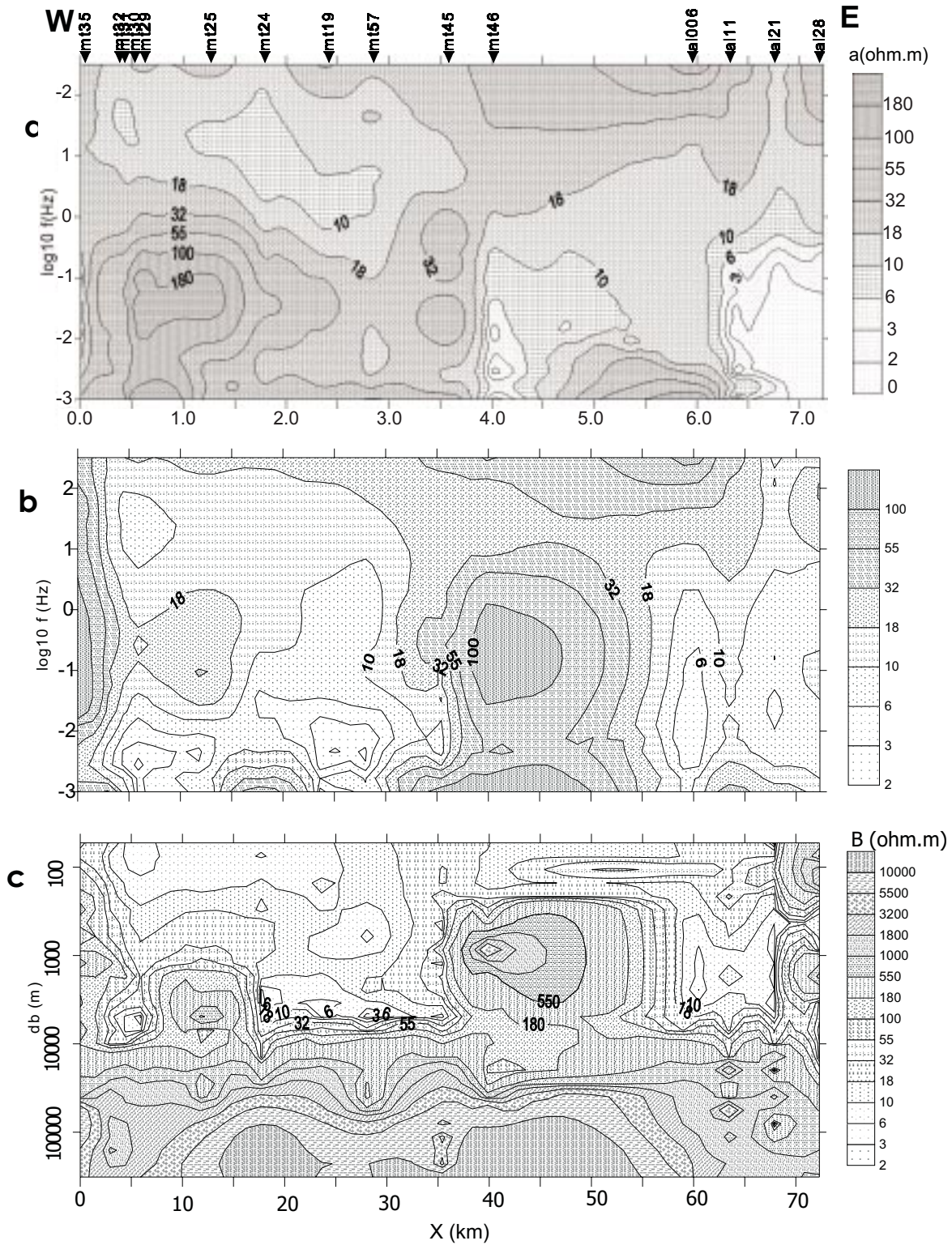


Figure 2. The MT apparent resistivity-frequency ( $\rho_a$ ,  $f$ ) pseudosections in (a) N-S, (b) E-W directions, and (c) Bostick resistivity-depth ( $\rho_b$ ,  $db$ ) transformation of the E-W apparent resistivity data along profile M1.

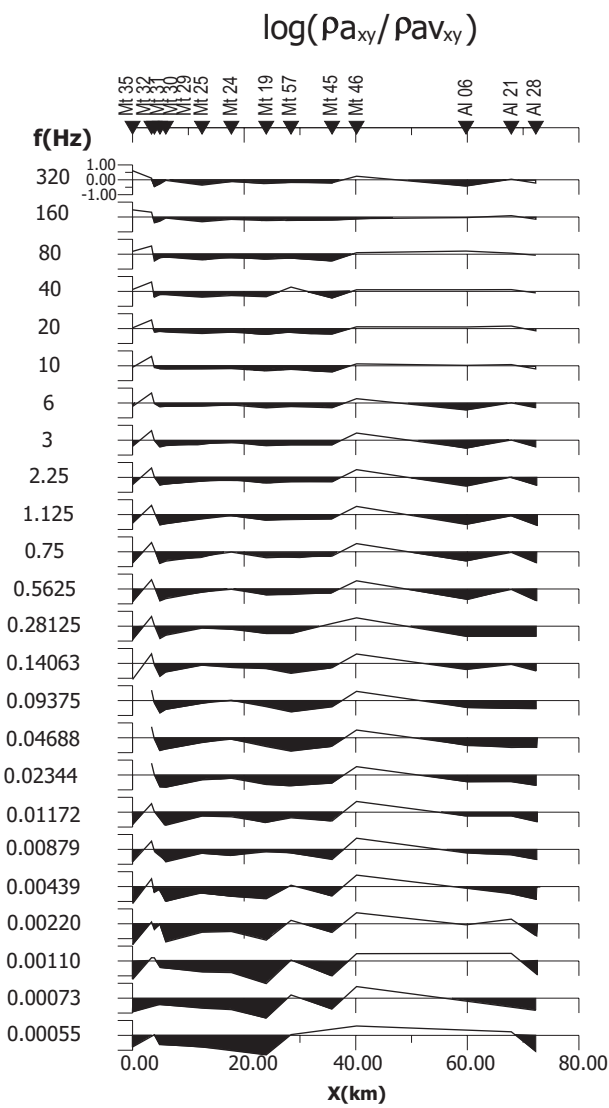


Figure 3. Profiles of logarithm of residual resistivity at 24 fixed frequencies at 14 stations along the N-S direction.

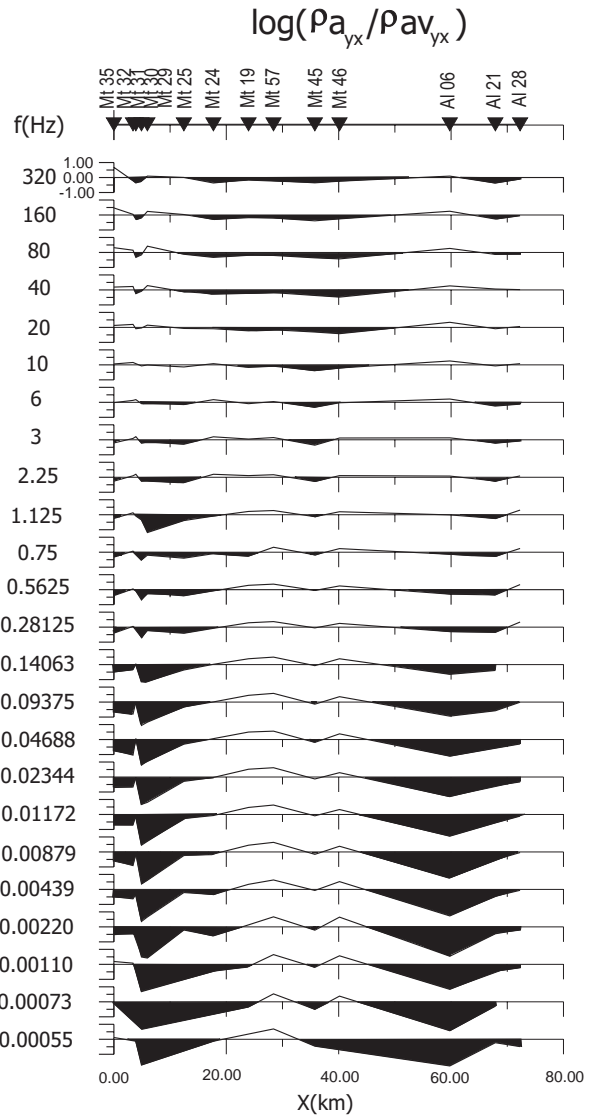
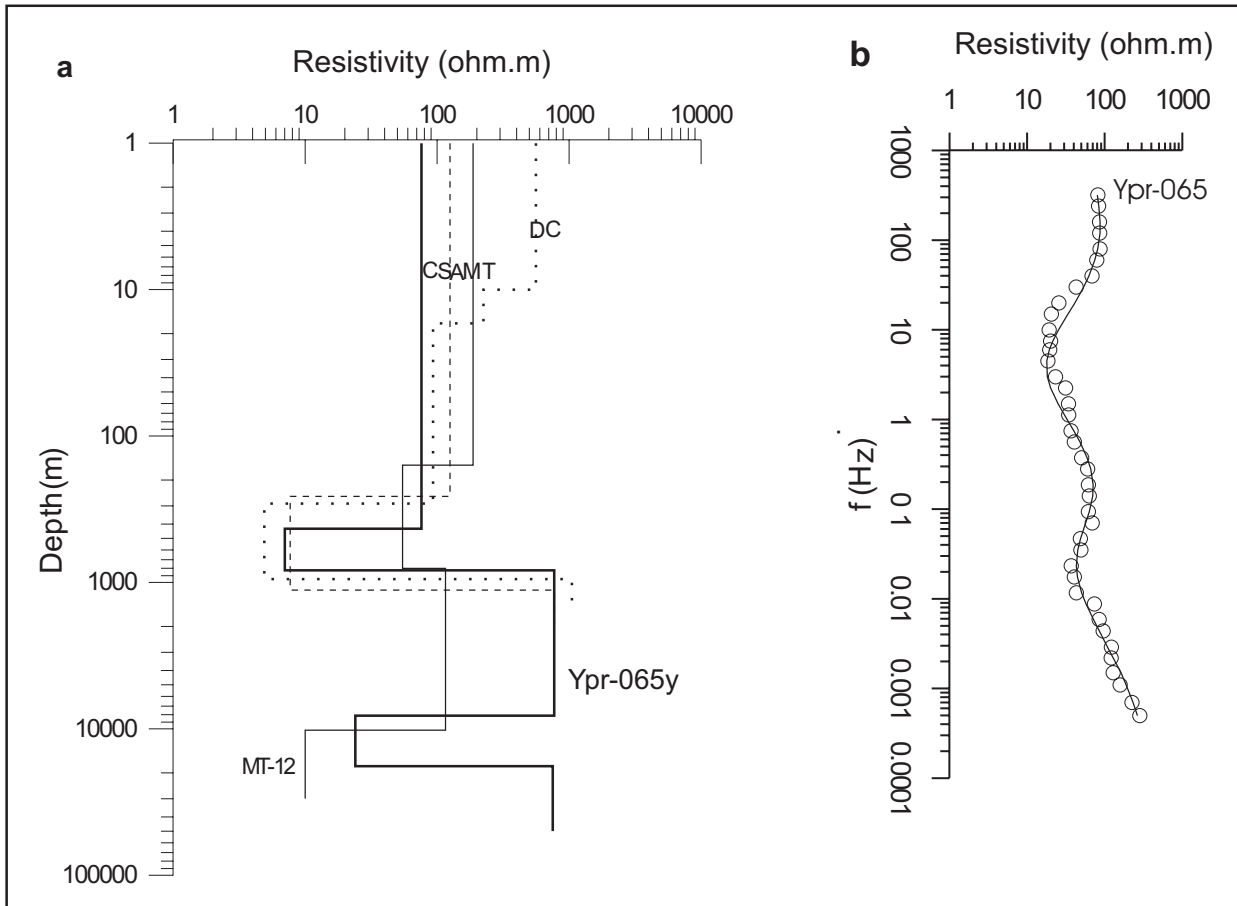


Figure 4. Profiles of logarithm of residual resistivity at 24 fixed frequencies at 14 stations along the E-W direction.

### Discussion

In this study, MT data from the M1 and M2 lines (that are approximately parallel and perpendicular to the major axis of the Gediz graben, respectively) are presented. The resistivity distribution versus the depth and distance are obtained using Bostick transformation (Figure 2). The resistivity distribution along profile M1 showed an undulating resistive basement under the conductive sedimentary cover along the graben. There are sudden interruptions in the lateral continuity of resistivity in Bostick sections. The undulating basement topography on

Bostick sections is formed and stressed by these abrupt lateral changes in resistivity. The MT data were also presented as residual apparent resistivity profiles (Figures 3 and 4) to clarify possible lateral resistivity boundaries. Residual resistivity profiles show deviation of resistivity at a certain site from the average resistivity obtained from all sites for any frequency in the region. Strong peaks (negative and positive anomalies) show that resistivity is anomalously different near this site compared to the environs. Such a difference in resistivity may be caused by any lithology change at this site or, less plausibly, any



**Figure 5.** (a) 1D inversion results from co-located DC (Direct Current) resistivity, CSAMT (Controlled Sourced Audio Frequency Magnetotelluric), and MT (Magnetotelluric) soundings from sites MT-12 and ypr-65; and (b) The actual response of the Earth to the sounding at MT site ypr-65 (circles) and the best-fit model response (solid curve) to the field data.

lateral variation of the physical conditions in the same lithology. So, the resistivity variations on both the residual apparent resistivity and Bostick sections along E-W profile M1 may be indicators of any hidden faults perpendicular to the profile.

High tipper values at most of the MT sites and high skew at some sites (except the MT19- MT 57) shows that the region is at least two dimensional in the Gediz graben. Therefore a detailed two-dimensional modelling is necessary to see the exact boundaries of basement topography and upper-lower crust in the region. We present the total thickness of the sedimentary formations (with different low resistivity layers) based on 1D inversion for some sites along M1 line in Table 1. The resistance of the sedimentary units (sum of the thickness and resistivity products of each layer in the sequence) and

resistance of crystalline basement (product of the thickness and resistivity of the basement) are also presented in the table. The results indicate that the thickness of the sediments changes from 934 m to 3817 m along the graben. Sarı and Şalk (1995) also estimated the thickness of the sediments as 2.5 km on a profile crossing the Gediz graben near Salihli via modelling of gravity data.

It is known that the lower crust is mostly conductive in Phanerozoic regions. In this study, we have identified this conductive zone (10 ohm.m) at 10-km-depth in the Gediz graben. This zone is quite shallow in the region as compared to a depth of 26 km in the northwestern Anatolia (Gölpazarı) region (Gürer 1996). According to İlkışık (1995), the heat flow in the region is 50% higher than the world average. The maximum heat-flow values

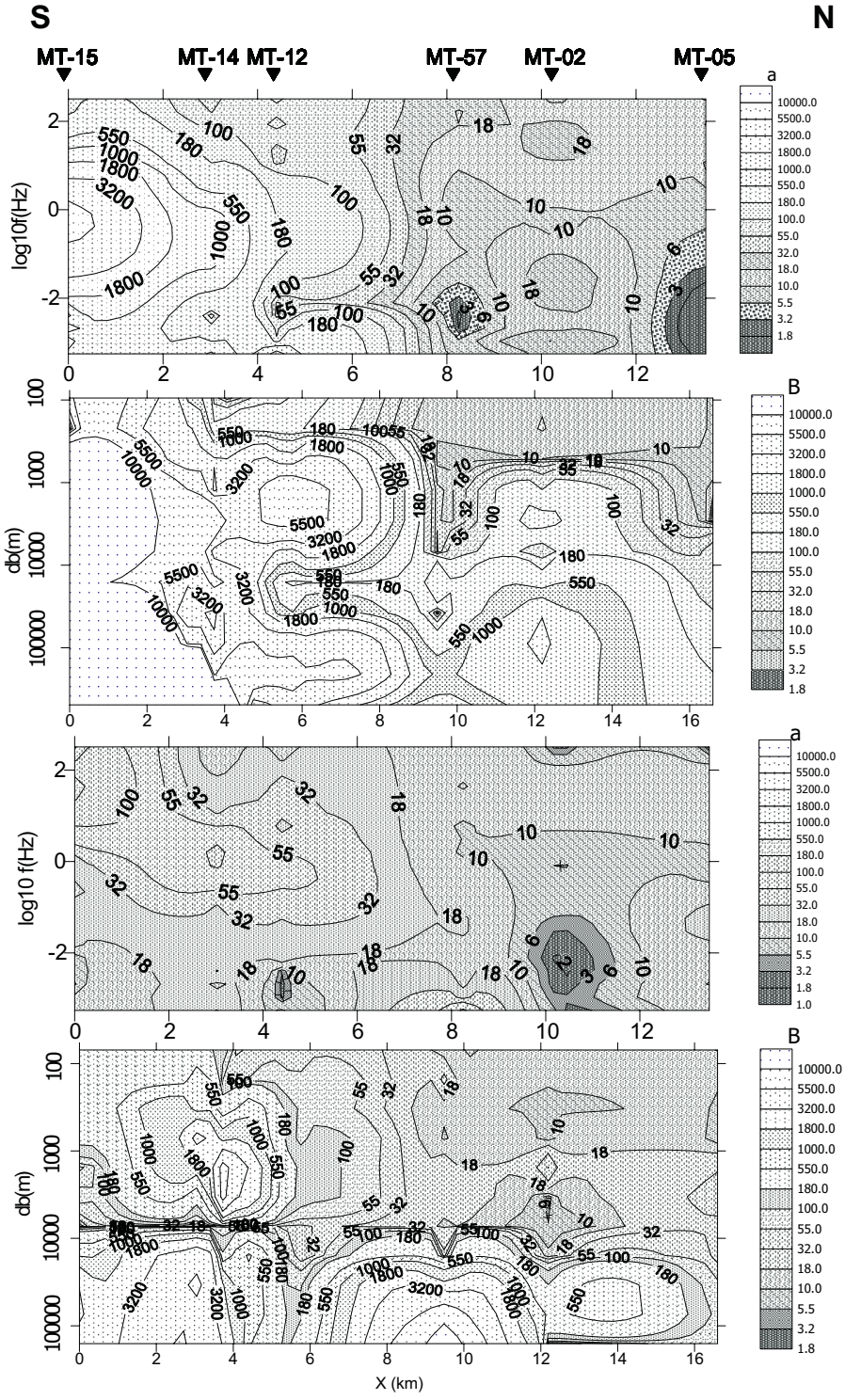


Figure 6. (a) MT apparent resistivity pseudosections in the E-W direction; (b) its Bostick depth transformation in the E-W direction; (c) The MT apparent resistivity pseudosections in the N-S direction; and (d) its Bostick depth transformation in the N-S direction along profile M2.

**Table 1.** Total thickness of sedimentary layers that cover the basement rocks in the Gediz graben for some sites along M1 line, based on 1D inversion.  $h$  denotes the depth to the basement.  $R_{sed}$  and  $R_{bas}$  show resistance of the sedimentary fill and basement, respectively.

MT site	MT31	MT30	MT29	MT25	MT24	MT19	MT57	MT45
$h(m)$	1963	1053	1807	3444	3314	1219	934	3817
$R_{sed}$	2446	49029	104731	264297	101861	10936	12259	16314
$R_{bas}$	870210	2093225	26471160	591039676	76692616	251117	237398	102410

of the western Anatolian graben systems are observed around the Gediz and neighbouring Büyük Menderes grabens (120-300 mW/m<sup>2</sup>). In extensional tectonic regimes, the foci of earthquakes are generally at depths between 8-12 km (Lister & Davis 1989) because the rocks become ductile at greater depths. This depth is in agreement with the depth to the conductive zone in the crust that we have identified in our study. The reason that lower crustal conductivity is observed in many regions of the world is still under discussion. This conductivity is mainly explained by possible high water or graphite content in the lower crust (Jones 1987), or by partial melting in the crust in extensional regions where the heat flow is higher than 85 mW/m<sup>2</sup> (Adam 1987). In regions where heat flow is considerably higher than the world average, this conductive zone is shallower than the world average (15-20 km). If we consider the extensional regime (Şengör *et al.* 1984; Seyitoğlu 1997; Yılmaz *et al.* 2000) of western Anatolia and high regional heat flow (50% higher than the world average), the conductive zone at about 10-km-depth can be related to high temperatures in the lithosphere and thinned crust around the Gediz graben.

## References

- ADAM, A. 1987. Are there two types of the conductivity anomaly caused by fluid in the crust? *Physics of the Earth and Planetary Interiors* **45**, 209-215.
- BAYRAK, M., İLKIŞIK, O.M., KAYA, C. & BAŞOKUR, A.T. 2000. Magnetotelluric data in western Turkey dimensionality analysis using Mohr circles. *Journal of Geophysical Research* **105**, B10, 23391.
- BAŞOKUR, A.T., İLKIŞIK, O.M., TOKGÖZ, T., KAYA, C., ULUGERGERLİ, E.U., GÜNER, A., DUVARCI, E., BILGIN, ÇINAR, A., KONAK, N., BAYRAK, M., PEŞEN, E. & KARLIK, G. 1996. The investigation of the crustal structure of Aegean region by the magnetotelluric method. *Ulusal Deniz Jeolojisi ve Jeofiziği Programı 8-9 February, 1996*, 20-25.
- CAGNIARD, L. 1953. Basic theory of magnetotelluric method of geophysical prospecting. *Geophysics* **18**, 605-634.
- COHEN, H.A., DART, C.J., AKYÜZ, H.S. & BARKA, A. 1995. Syn-rift sedimentation and structural development of the Gediz and Büyük Menderes graben, western Turkey. *Journal of the Geological Society, London* **152**, 529-638.
- GÜNER, A. 1996. Deep conductivity structure of the North Anatolian Fault zone and the Istanbul and Sakarya Zones along the Gölpaazarı-Akçaova profile, northwest Anatolia. *International Geology Review* **38**, 727-736.
- İLKIŞIK, O.M. 1995. Regional heat flow in western Anatolia using silica temperature estimates from thermal springs. *Tectonophysics* **244**, 175-184.

## Conclusions

In this study we analysed and interpreted geoelectrical (mainly MT) data from the Gediz graben. The results show a rugged basement topography and varying sediment thickness along the graben (~950-3800 m). The abrupt lateral changes in resistivity in the E-W direction under the surface cover of the graben may be related to vertical geological contacts. Conductive lower crust is identified at a depth of 10 in the Gediz graben. The conductive zone is more shallow in the region as compared to that in northwestern Anatolia. This situation may have been caused by thinning and high regional heat flow in the crust of western Anatolia.

## Acknowledgements

This study was supported by the Research Fund of İstanbul University project numbers: 842/190496 and Ö-326/030697. We are also thankful to TPAO for their kind permission for the use of their data in this research. We would like to thank anonymous reviewers for their constructive comments that improved the earlier version of the text. Steven K. Mittwede helped with the English.

- İLKİŞİK, O.M. & YENİGÜN, H.M. 1997: Heat flow data and shallow thermal regime in western Turkey. *Abstracts, İstanbul 97 International Geophysical Conference & Exposition, sponsored, SEG, EAGE, Chamber of Geophysical Engineers of Turkey*, 74.
- JONES, A.G. 1987. MT and reflection: an essential combination. *Geophysical Journal of Royal Astronomical Society* **89**, 7-18.
- KOÇYİĞİT, A., YUSUFOĞLU, H. & BOZKURT, E. 1999. Evidence from the Gediz Graben for episodic two-stage extension in western Turkey. *Journal of the Geological Society, London* **156**, 605-616.
- LISTER, G.S. & DAVIS, G.A. 1989. The origin of metamorphic core complexes and detachment faults formed during Tertiary continental extension in the northern Colorado River region, USA. *Journal of Structural Geology* **11**, 65-94.
- MTA 1964. *Geological Map of Turkey, Scale 1:500 000. İzmir Sheet*. Institute of Mineral Research and Exploration Publications, Ankara.
- SARI, C. & ŞALK, M. 1995. Estimation of the thickness of the sediments in the Aegean grabens by 2-D and 3-D analysis of the gravity anomalies. *International Earth Sciences Colloquium on the Aegean Region, IESCA, Güllük October 9-14 Turkey*, 255-273.
- SEYİTOĞLU, G. & SCOTT, B.C. 1992. The age of Büyük Menderes Graben (west Turkey) and its tectonic implications. *Geological Magazine* **129**, 239-242.
- SEYİTOĞLU, G. & SCOTT, B.C. 1994. Late Cenozoic basin development in west Turkey: Gördes basin: tectonics and sedimentation. *Geological Magazine* **131**, 631-637.
- SEYİTOĞLU, G. & SCOTT, B.C. 1996. The age of the Alaşehir graben (west Turkey) and its tectonic implications. *Geological Journal* **31**, 1-11.
- SEYİTOĞLU, G. 1997. Late Cenozoic tectono-sedimentary development of Seli and Uşak-Güre basins: a contribution to the discussion on the development of east-west and north-trending basins in western Turkey. *Geological Magazine* **134**, 163-175.
- ŞENGÖR, A.M.C. 1987. Cross-faults and differential stretching of hanging wall in regions of low angle normal faulting: examples from Western Turkey. In: COWARD, M.P., DEWEY, J.F., HANCOCK, P.L. (eds), *Continental Extensional Tectonics*. Geological Society of London, Special Publications **28**, 575-589.
- ŞENGÖR A.M.C., SATIR M. & AKKÖK R. 1984. Timing of tectonic events in the Menderes Massif, western Turkey: implications for tectonic evolution and evidence for Pan-African basement in Turkey. *Tectonics* **3**, 693-707
- STERNBERG B.K., WASHBURNE J.C. & PELLERIN L. 1988. Correction for the static shift in magnetotellurics using transient electromagnetic soundings. *Geophysics* **53**, 1459-1468.
- WESTAWAY, R. 1994. Evidence for dynamic coupling of surface processes with isostatic compensation in the lower crust during active extension of western Turkey. *Journal of Geophysical Research* **99**, 20203-20223.
- YILMAZ, Y., GENÇ, Ş.C., GÜRER, Ö.F., BOZCU, M., YILMAZ, K., KARACIK, Z., ALTUNKAYNAK, Ş. & ELMAS, A. 2000. When did the western Anatolian grabens begin to develop. In: BOZKURT, E., WINCHESTER, J.A. & PIPER, J.D.A. (eds), *Tectonics and Magmatism in Turkey and the Surrounding Area*. Geological Society of London, Special Publications **173**, 353-384.

Received 26 February 2001; revised typescript accepted 19 October 2001